

## Article

# Separation of Cesium and Rubidium from Solution with High Concentrations of Potassium and Sodium

Junjie Xie <sup>1</sup>, Kang Li <sup>1</sup>, Zhuonan Shi <sup>1</sup>, Changli Min <sup>1</sup>, Shina Li <sup>2</sup>, Zichen Yin <sup>1</sup> and Ruixin Ma <sup>1,3,\*</sup>

<sup>1</sup> School of Metallurgical and Ecological Engineering, University of Science and Technology Beijing, Beijing 100083, China

<sup>2</sup> Tianjin Research Institute of Water Transport Engineering, Ministry of Transport, Tianjin 30000, China

<sup>3</sup> Beijing Key Laboratory of Special Melting and Preparation of High-End Metal Materials, Beijing 100083, China

\* Correspondence: maruixin@ustb.edu.cn

**Abstract:** Solvent extraction with 4-tert-butyl-2-( $\alpha$ -methylbenzyl) phenol (t-BAMBP) is an effective method for the separation and purification of rubidium and cesium. A solution containing a high  $K^+$  concentration (exceeding 80 g/L), which was ultra-salty, with about 200 g/L alkali metal ions, was used to extract  $Rb^+$  and  $Cs^+$ . The effects of the process parameters on the separation of cesium and rubidium were systematically studied. The optimum conditions were as follows: NaOH concentration of 0.5 mol/L, t-BAMBP concentration of 1 mol/L (in sulfonated kerosene), organic/aqueous volume ratio (O/A ratio) of 3:1, and contact time of 1 min. The extraction rates of cesium and rubidium were 99.81 and 98.09%, respectively, and 19.31% of potassium was co-extracted in the organic phase after five-stage countercurrent extraction. About 99.32% of  $K^+$  in the organic phase could be removed after five-stage countercurrent scrubbing with deionized water at an O/A ratio of 2:1 for 2 min. When 0.5 mol/L hydrochloric acid solution was used as detergent, almost all of the cesium and rubidium (>99%) could be recovered by two-stage countercurrent stripping at an O/A ratio of 3:1 for 2 min. A solid compound was found and collected from the organic phase during multi-stage solvent extraction. Its composition and structure were determined by XRD, infrared Fourier-transform, and ICP-MS.

**Keywords:** t-BAMBP; rubidium; cesium; potassium; extraction complex



**Citation:** Xie, J.; Li, K.; Shi, Z.; Min, C.; Li, S.; Yin, Z.; Ma, R. Separation of Cesium and Rubidium from Solution with High Concentrations of Potassium and Sodium. *Separations* **2023**, *10*, 42. <https://doi.org/10.3390/separations10010042>

Academic Editor: Gavino Sanna

Received: 19 December 2022

Revised: 5 January 2023

Accepted: 6 January 2023

Published: 9 January 2023



**Copyright:** © 2023 by the authors. Licensee MDPI, Basel, Switzerland. This article is an open access article distributed under the terms and conditions of the Creative Commons Attribution (CC BY) license (<https://creativecommons.org/licenses/by/4.0/>).

## 1. Introduction

Cesium and rubidium are strategic metals and have been widely used in catalysts [1], special glass [2], and medicine [3]. With the development of modern technology, rubidium and cesium play indispensable roles in perovskite solar cells [4–6], magnetofluidic power generation [7], and spacecraft [8]. The extraction of cesium and rubidium mainly depends on the solid minerals used, such as lepidolite and pollucite [9–12]. After being treated by roasting and leaching processes, rubidium and cesium can be transformed into solution.

The methods used for the separation and purification of  $Rb^+$  and  $Cs^+$  include precipitation, solvent extraction, and ion exchange [13]. Precipitation [14,15] is not-widely used because of the poor separation performance, high reagent price, and complicated separation process. Ion exchange [16–19] is mainly used for the separation or enrichment of  $Rb^+$  and  $Cs^+$  due to its low adsorption capacity. On the other hand, solvent extraction [20–25], based on the advantages of fast reaction, simple operation, and high separation performance, is regarded as the most promising method for the separation and purification of  $Rb^+$  and  $Cs^+$  from relatively high-concentration solutions. The extractants for  $Rb^+$  and  $Cs^+$  are mainly substituted phenol or crown ether [26,27]. Substituted phenolics [28–32], such as 4-tert-butyl-2-( $\alpha$ -methylbenzyl) phenol (t-BAMBP) and 4-s-butyl-2-( $\alpha$ -methylbenzyl) phenol (BAMBP), are widely used for the separation and purification of

Rb<sup>+</sup> and Cs<sup>+</sup> because of their high selectivity, low price, rapid reaction, and high cycle performance. The sequence of alkali metal extraction by t-BAMBP and BAMBP is in the order of Cs<sup>+</sup> > Rb<sup>+</sup> > K<sup>+</sup> > Na<sup>+</sup> > Li<sup>+</sup> [10,33].

The separation and purification of Cs<sup>+</sup> or Rb<sup>+</sup> is difficult due to their similar chemical properties to K<sup>+</sup>, Rb<sup>+</sup>, and Cs<sup>+</sup>, which often co-exist with each other [13]. According to Liu et al. [23], the presence of Mg<sup>2+</sup> and K<sup>+</sup> has a significant influence on the extraction of Rb<sup>+</sup> and Cs<sup>+</sup>. Ross et al. [33] investigated the influence of sodium salts on the extraction performance of BAMBP, and the results indicated that sodium salts, especially high concentrations of sodium hydroxide, reduced the extractability of rubidium and cesium. Horner et al. [33] noted that BAMBP molecules form a relatively water-soluble species with sodium, which has a detrimental effect on extraction and causes reagent loss. Therefore, when there are high concentrations of K and Na in the feed solution (7.71 g/L Cs<sup>+</sup>, 6.54 g/L Rb<sup>+</sup>, 82.18 g/L K<sup>+</sup>, 86.13 g/L Na<sup>+</sup>), it is necessary to determine a suitable condition for the separation of rubidium and cesium from the potassium and sodium. Table S1 (Supplementary Materials) lists the studies on separating cesium and rubidium in recent years. As shown in the table, most research has focused on the separation of low concentrations of cesium and rubidium from brine, while few studies have focused on the separation of high concentrations of cesium and rubidium from feed solution with ultra-high concentrations of potassium and sodium. Based on the above analysis, the process of separating cesium and rubidium from high salt solutions was studied in order to realize the utilization of cesium and rubidium resources.

Generally, the diluent has a definite effect on the extraction and phase separation process. Currently, the diluents used for t-BAMBP include sulfonated kerosene, xylene, carbon tetrachloride, and cyclohexane. Among these diluents, the most studied is sulfonated kerosene because of its low toxicity, non-volatilization, and low price [10]. Thus, sulfonated kerosene was selected as the diluent for the separation of cesium and rubidium in this study.

To the best of the authors' knowledge, there are few studies on the selective extraction of Cs<sup>+</sup> and Rb<sup>+</sup> from feed solution with ultra-high concentrations (>80 g/L) of K<sup>+</sup>, especially with an ultra-high content of about 200 g/L alkali metal ions. In this study, the effects of parameters on the extraction rates of K<sup>+</sup>, Rb<sup>+</sup>, and Cs<sup>+</sup> were systematically investigated. In addition, the formation of the solid compound during extraction was also studied. The results are significant for the separation and purification of Rb<sup>+</sup> and Cs<sup>+</sup> from solutions with high concentrations of K<sup>+</sup> and Na<sup>+</sup>.

## 2. Materials and Methods

### 2.1. Materials

The feed solution was provided by a company in Hebei Province, China. The element concentrations are shown in Table 1.

**Table 1.** Concentrations of elements in the feed solution.

Element	Na	K	Rb	Cs	Cl	Br	I
Concentration (g/L)	86.13	82.18	6.54	7.71	191.39	20.98	40.99

The extractant was t-BAMBP with a purity of >93%, and the diluent was sulfonated kerosene, purchased from Beijing RLK Separation Technology Co., Ltd. (Beijing, China). The chemical reagents (analytical reagent grade), sodium hydroxide and hydrochloric acid, were purchased from Shanghai Aladdin Biochemical Technology Co., Ltd. (Shanghai, China).

### 2.2. Experimental Procedure

The solvent extraction experiments were conducted at room temperature (20 ± 2 °C) using separating funnels. The organic phase consisted of sulfonated kerosene and t-BAMBP

(t-BAMBP concentration was 0.25–1.5 mol/L). Sodium hydroxide was added to the feed solution before extraction (NaOH concentration was 0.1–1.5 mol/L). The aqueous phase was mixed with the organic phase in a certain O/A ratio (organic /aqueous volume ratio was 1:2–4:1), and shaken for a period of time (contact time was 1–5 min). After the separation of the two phases, the concentration of alkali metal in the aqueous was measured by ICP or ICP-MS, and the alkali metal concentration in the organic phase was calculated by element conservation.

The extraction rates of K, Rb, and Cs ( $E_K$ ,  $E_{Rb}$ , and  $E_{Cs}$ ) and the separation factor of Rb/K ( $\beta_{Rb/K}$ ) were calculated by Equations (1) and (2):

$$E = \left( 1 - \frac{C_{aq}V_{aq}}{CV} \right) \times 100\% \tag{1}$$

$$\text{separation factor}(\beta_{Rb/K}) = \frac{[Rb]_{org} \times [K]_{aq}}{[Rb]_{aq} \times [K]_{org}} \tag{2}$$

where  $C_{aq}$  and  $C$  represent the concentration of alkali metal in the raffinate and feed solution (g/L), respectively;  $V_{aq}$  and  $V$  represent the volume of the raffinate and feed solution (L), respectively;  $[Rb]_{org}$  and  $[K]_{org}$  refer to the respective concentration of rubidium and potassium in organic phase (g/L); and  $[Rb]_{aq}$  and  $[K]_{aq}$  refer to the concentration of rubidium and potassium, respectively, in aqueous phase (g/L).

### 2.3. Chemical Analysis

The contents of cesium and rubidium in the raffinate were measured by inductively coupled plasma mass spectrometry (ICP-MS; Agilent-7800, Agilent Technologies Inc., Palo Alto, CA, USA). The concentrations of other elements, including sodium, potassium, and iodine, were analyzed by inductively coupled plasma optical emission spectrometry (ICP-OES; Agilent-725, Agilent Technologies Inc., Palo Alto, Santa Clara, CA, USA). The concentration of chloride ions was measured by ion chromatography (IC; Dionex ICS-1100, Thermo Fisher Scientific, Waltham, MA, USA). Fourier-transform infrared spectroscopic analysis of the organic phase was carried out on an infrared spectrometer (FT-IR; Nicolet IS10, Nicolet, Madison, WI, USA) with a scanning range of 400 to 4000  $\text{cm}^{-1}$ . The composition of the solid compound was determined by X-ray diffraction (XRD; Ultima IV, Rigaku, Tokyo, Japan).

## 3. Results and Discussion

### 3.1. Solvent Extraction of Cs and Rb

#### 3.1.1. Effect of NaOH Concentration on $E_K$ , $E_{Rb}$ , and $E_{Cs}$

According to previous research [23,24], t-BAMBP is a weakly acidic extractant, and its extraction mechanism is realized through the exchange of ions between hydrogen on the phenol hydroxyl group and alkali metals. The extraction process can be expressed by Equation (3):



According to Ross et al. [33], adding an appropriate amount of sodium hydroxide (1 mol/L) is conducive to the extraction of cesium and rubidium, but a further increase in the sodium hydroxide concentration is harmful to the extraction process. The effect of the NaOH concentration on the extraction of potassium, rubidium, and cesium was investigated using a t-BAMBP concentration of 1 mol/L, an O/A ratio of 1:1, and a contact time of 2 min while varying the concentration of sodium hydroxide from 0.1 to 1.5 mol/L. According to previous studies [25,34], the extraction rate of cesium ( $E_{Cs}$ ) and rubidium ( $E_{Rb}$ ) increased with the increasing sodium hydroxide concentration between 0 and 1 mol/L. However, due to the high concentration of  $\text{Na}^+$  in the feed solution, which interferes somewhat with the extraction process, both  $E_{Cs}$  and  $E_{Rb}$  decreased when the NaOH concentration exceeded only 0.5 mol/L. The experimental results are shown in Figure 1a. The extraction rate of cesium ( $E_{Cs}$ ) increased rapidly with solution alkalinity from 0 to 0.5 mol/L, reaching a maximum of 90.53% at a NaOH concentration of 0.5 mol/L, and then slightly decreased above 0.5 mol/L. The extraction rate of rubidium ( $E_{Rb}$ ) increased rapidly

with sodium hydroxide concentration from 0 to 0.5 mol/L and then increased slightly, reaching a maximum of 38.63% at a NaOH concentration of 1 mol/L. Different from rubidium and cesium, the extraction rate of potassium ( $E_K$ ) increased slowly as the sodium hydroxide concentration increased from 0 to 1.5 mol/L, reaching a maximum of 12.05% at a NaOH concentration of 1.5 mol/L. With increased sodium hydroxide concentration, the separation factor of Rb/K ( $\beta_{Rb/K}$ ) first increased and then decreased; the maximum  $\beta_{Rb/K}$  was 15.88 at a NaOH concentration of 0.5 mol/L. Obviously, a large separation factor of Rb/K is beneficial to the separation of cesium and rubidium. Therefore, a NaOH concentration of 0.5 mol/L was selected as the optimum condition for the separation of cesium and rubidium.

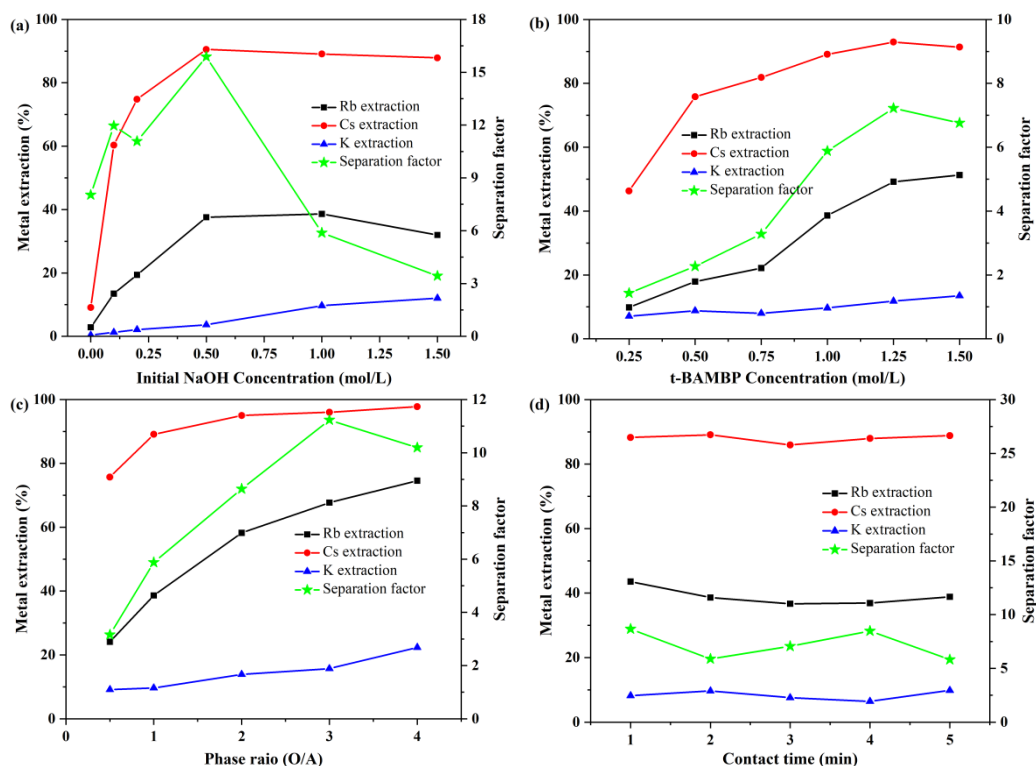


**Figure 1.** Effect of (a) NaOH concentration, (b) t-BAMBP concentration, (c) O/A ratio, and (d) contact time on metal extraction by the t-BAMBP/sulfonated kerosene system.

### 3.1.2. Effect of the t-BAMBP Concentration on $E_K$ , $E_{Rb}$ , and $E_{Cs}$

It is well known that the extractant concentration is related to the extraction capacity [23]; thus, increasing the concentration of the extractant is usually beneficial to the extraction process. Figure 1b shows  $E_K$ ,  $E_{Rb}$ , and  $E_{Cs}$  at different t-BAMBP concentrations. Other conditions were unchanged: NaOH concentration of 1 mol/L, O/A ratio of 1:1, and contact time of 2 min. With increased t-BAMBP concentration,  $E_{Cs}$  increased rapidly with extractant concentration from 0.25 to 1.25 mol/L and then slightly decreased at 1.5 mol/L.  $E_{Rb}$  and  $E_K$  showed an upward trend as the extractant concentration increased from 0.25 to 1.5 mol/L, reaching a maximum of 51.28 and 13.48%, respectively. Similar to the cesium extraction curve, the separation factor curve of Rb/K first increased and then decreased with increased extractant concentration and reached a maximum of 7.22 when the extractant concentration was 1.25 mol/L. According to the experimental results, an ultra-high concentration of t-BAMBP was not conducive to extraction. In addition, the viscosity of the organic phase also increased with t-BAMBP concentration, which could cause problems such as poor separation performance and even emulsification. In view of the above findings, a t-BAMBP extractant concentration of 1 mol/L in sulfonated kerosene was considered to be the optimal condition.

### 3.1.3. Effect of the O/A Ratio on $E_K$ , $E_{Rb}$ , and $E_{Cs}$

To investigate the effect of the O/A ratio on the extraction of metals, sulfonated kerosene containing 1 mol/L t-BAMBP was mixed with feed solution containing 1 mol/L NaOH at different volume ratios for 2 min. The experimental results were the same as those of Li et al. [24]: the metal extraction rate increased with the O/A ratio due to the increased relative availability of t-BAMBP. As can be seen in Figure 1c, the extraction rates of Cs, Rb, and K increased as the O/A ratio increased from 1:2 to 4:1, reaching maximum values of 97.77, 74.58, and 22.36%, respectively, at an O/A ratio of 4:1. Among these alkali metals,  $E_{Rb}$  changed obviously, showing a significant increase from 24.13 to 74.58%, while  $E_K$  increased from 9.15 to 22.36%.  $\beta_{Rb/K}$  increased rapidly as O/A ratio changed from 1:2 to 3:1 and then decreased slightly at an O/A ratio of 4:1, and the maximum  $\beta_{Rb/K}$  was 11.23 at an O/A ratio of 3:1. Generally, a high  $\beta_{Rb/K}$  value is beneficial for subsequent scrubbing of potassium; thus, an O/A ratio of 3:1 was determined as the optimal separation condition.

### 3.1.4. Effect of the Contact Time on $E_K$ , $E_{Rb}$ , and $E_{Cs}$

According to the reaction kinetics, increasing the contact time is beneficial to the ion exchange between the alkali metal and t-BAMBP molecules. In order to determine the appropriate contact time for extraction, the experiments were performed under the following conditions: 1 mol/L NaOH, 1 mol/L t-BAMBP (in sulfonated kerosene), O/A ratio of 1:1, and contact time of 1–5 min. As shown in Figure 1d, the extraction rates of the alkali metals showed little change with increased contact time. The results indicate that the extraction reaction reached equilibrium within a short period, which was beneficial for the separation process. The separation factor of Rb/K changed slightly with increased contact time, and  $\beta_{Rb/K}$  reached a maximum of 8.66 at a contact time of 1 min. Therefore, a contact time of 1 min was considered to be the optimal condition for the efficient separation of rubidium and potassium.

According to the above analysis, the optimal conditions for the separation of cesium and rubidium from the feed solution with high concentrations of potassium and sodium are as follows: NaOH concentration of 0.5 mol/L, t-BAMBP extractant concentration of 1 mol/L (in sulfonated kerosene), O/A ratio of 3:1, and contact time of 1 min.

### 3.1.5. Extraction Isotherm of Rb

A McCabe-Thiele diagram is commonly used to predict the theoretical extraction stage [30]. The extraction isotherm of rubidium was constructed using O/A ratios of 1:2, 1:1, 2:1, 3:1, and 4:1, and the results are shown in Figure 2. The extraction isotherm diagram predicted that the concentration of rubidium in the feed solution would be reduced to 0.146 g/L, corresponding to  $E_{Rb}$  reaching 97.77%, after five-stage countercurrent extraction at an O/A ratio of 3:1.

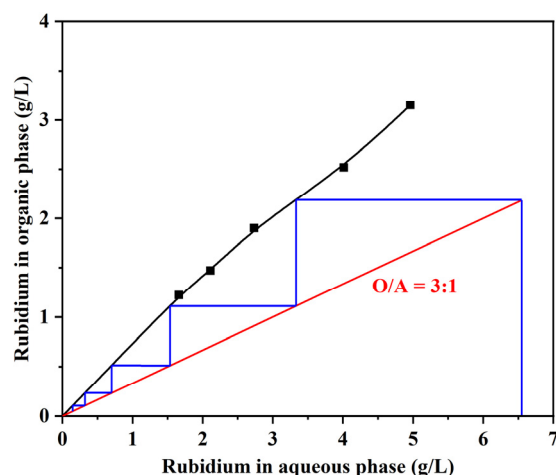


Figure 2. Extraction isotherm of Rb.

To assess the accuracy of prediction, a five-stage countercurrent extraction simulation experiment was conducted under the proper conditions: NaOH concentration of 40 g/L, extractant concentration of 1 mol/L, O/A ratio of 3:1, and 2 min contact time. After solvent extraction with t-BAMBP, the concentrations of cesium and rubidium in the feed solution decreased to 0.015 and 0.125 g/L, respectively, corresponding to  $E_{Cs}$  of 99.81% and  $E_{Rb}$  of 98.09%. However, about 19.31% of impure potassium was extracted into the organic phase, corresponding to the concentration of potassium in organic phase reaching 5.29 g/L.

### 3.2. Scrubbing of K

After multistage extraction, the obtained organic phase contained 2.57 g/L cesium and of 2.14 g/L rubidium, as well as a high concentration of impure potassium (5.29 g/L). Obviously, the impure potassium in the organic phase needed to be further removed. According to Xing et al. [25], deionized water is an effective scrubbing agent for the removal of potassium.

#### 3.2.1. Effect of the O/A Ratio on $K^+$ , $Rb^+$ , and $Cs^+$ Scrubbing

In order to determine the appropriate conditions for potassium scrubbing, a series of scrubbing experiments were conducted at room temperature under different O/A ratios. As shown in Figure 3, it is obvious that the metal scrubbing rates were in the order of  $K > Rb > Cs$  under the same conditions, which was opposite to the order of metal extraction. In addition, with increased O/A ratio, the scrubbing rates of cesium, rubidium, and potassium decreased due to the decrease in deionized water consumption. Among these alkali metals, the scrubbing rate of cesium was slightly affected by the change in the O/A ratio, decreasing only from 7.27 to 5.56%, while the scrubbing rate of potassium was significantly affected by the change in the O/A ratio, decreasing from 92.69 to 55.64%. In addition, the separation factor of Rb/K also decreased when the O/A ratio increased from 1:2 to 4:1, and the maximum  $\beta_{Rb/K}$  reached 14.72 when the O/A ratio was 1:2. However, a small O/A ratio requires high water consumption, resulting in a significantly increased production cost. After comprehensive consideration, an O/A ratio of 2:1 with a separation factor of 8.05 was used for potassium scrubbing.

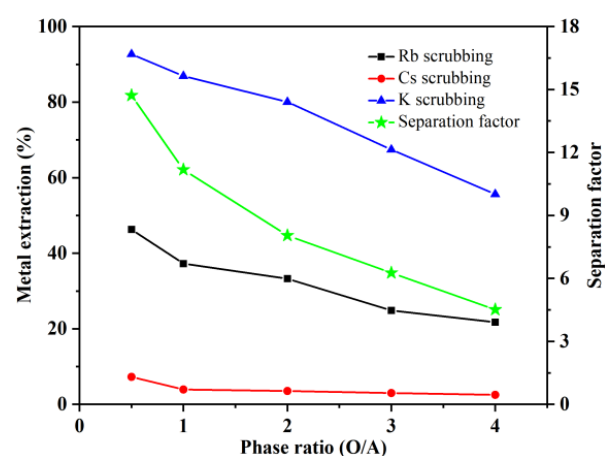


Figure 3. Effect of the O/A ratio on metal scrubbing by deionized water.

#### 3.2.2. Scrubbing Isotherm of K

In order to remove impure potassium in the organic phase, the scrubbing isotherm of potassium was constructed based on the scrubbing results at different O/A ratios. The McCabe-Thiele curve of potassium scrubbing is shown in Figure 4. After five-stage scrubbing with deionized water at O/A ratio of 2:1, the concentration of potassium in the organic phase was reduced to 0.0527 g/L, corresponding to a scrubbing rate of 99%.

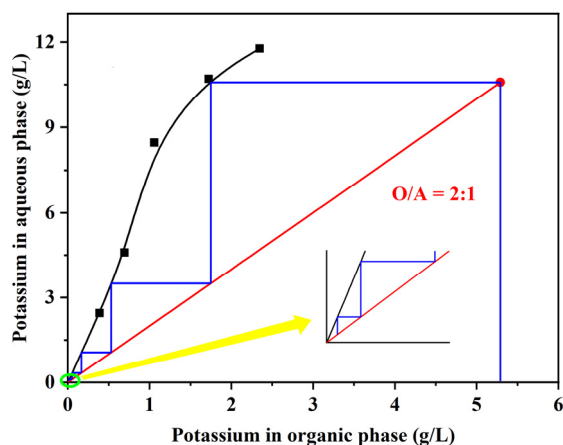


Figure 4. Scrubbing isotherm of K.

To verify this result, a five-stage countercurrent scrubbing simulation experiment was conducted under conditions of 2 min contact time and an O/A ratio of 2:1. After scrubbing with deionized water, the organic phase was scrubbed with 5 mol/L hydrochloric acid at an O/A ratio of 1:1 ratio for 2 min, and the concentration of potassium in the aqueous phase was 0.036 g/L, corresponding to a scrubbing rate of 99.32%.

### 3.3. Stripping of Cs and Rb

After the extraction and scrubbing stage, cesium and rubidium were successfully separated from potassium and sodium. In order to recover rubidium and cesium and realize the regeneration of the organic phase, the organic phase was exposed to hydrochloric acid solution. The influence of various factors on the recovery of Cs, Rb, and K was studied.

#### 3.3.1. Effect of HCl Concentration on K<sup>+</sup>, Rb<sup>+</sup>, and Cs<sup>+</sup> Stripping

Generally, a high concentration of hydrochloric acid is harmful to the organic phase; thus, the experiments were carried out at a low HCl concentration, less than 3 mol/L, and the other conditions were an O/A ratio of 1:1 and a contact time of 2 min. The experimental results are shown in Figure 5a. Under the same HCl concentration, the metal stripping rate was in the order of K > Rb > Cs, which was opposite to the metal extraction sequence. The metal stripping rates changed slightly with increased hydrochloric acid concentration, and more than 95% of Cs, Rb, and K was recovered in a single stripping stage. The results indicate that 0.5 mol/L hydrochloric acid solution was sufficient for stripping cesium and rubidium. In addition, a high concentration of hydrochloric acid will cause problems such as extractant degradation, and equipment corrosion. Therefore, 0.5 mol/L hydrochloric acid solution was used for the recovery of cesium and rubidium.

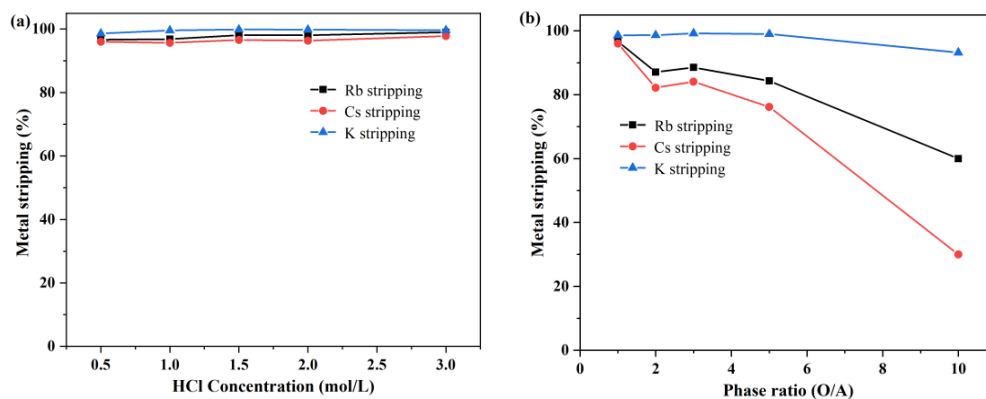


Figure 5. Effect of (a) the HCl concentration and (b) the O/A ratio on the stripping rates of K, Rb, and Cs.

### 3.3.2. Effect of the O/A Ratio on $K^+$ , $Rb^+$ and $Cs^+$ Stripping

The stripping experiments were conducted with 0.5 mol/L hydrochloric acid solution by changing the O/A ratio in a range of 1:1 to 10:1, and the result is shown in Figure 5b. With increased O/A ratio, the stripping rate of potassium decreased slightly, while the stripping rates of cesium and rubidium significantly decreased, reaching a minimum of 29.99 and 59.98%, respectively, at an O/A ratio of 10:1. When the O/A ratio was 3:1, 99.21% of potassium, 88.54% of rubidium, and 84.07% of cesium were stripped from the organic phase. As shown in Figure 5b, a small O/A ratio with high cesium and rubidium stripping rates was beneficial for metal recovery; however, the concentrations of cesium and rubidium in the stripping solution decreased with decreasing O/A ratio, which was not conducive to the subsequent separation and purification processes. Moreover, a small O/A ratio requires a large amount of stripping solution, which increases the loss of the organic phase and the cost. Based on these findings, an O/A ratio of 3:1 was determined to be the optimal stripping condition.

Finally, a two-stage countercurrent stripping simulation experiment was conducted under the following condition: contact time of 2 min, HCl concentration of 0.5 mol/L, and an O/A ratio of 3:1. The experimental results indicate that all potassium was stripped into the aqueous phase, and the stripping rates of Cs and Rb reached 99.61 and 99.36%, respectively.

### 3.4. Problems in the Extraction Process

In the multi-stage extraction process, the solid compound (Figure 6) formed in the organic phase, which seriously interfered with the extraction. In order to determine the reason for the formation of the solid compound, a series of tests were performed.



**Figure 6.** Morphology of the solid compound.

#### 3.4.1. XRD Patterns and ICP Analysis of the Solid Compound

The solid compound was dried at 120 °C to remove water and was then analyzed using an X-ray diffractometer. As can be seen in Figure 7, the characteristic peaks of NaCl and KCl appeared in the XRD patterns, while the characteristic peak of t-BAMBP was not obvious. Table 2 lists the chemical composition of the solid compound; the content of rubidium and cesium decreased after scrubbing, indicating that the solid compound was able to exchange ions with water. In addition, as shown in Figure 7, the sodium and potassium in the solid compound without scrubbing contained potassium chloride and sodium chloride, which came from the feed solution inclusions. Since t-BAMBP extractant has very low selectivity for sodium, it is assumed that all of the sodium in the solid compound (2.35%) came from the feed solution, corresponding to the inclusion potassium from the feed solution, calculated as 1.77%. Therefore, as shown in Table 2, about 0.89% K, 1.39% Rb, and 8.23% Cs were bound to t-BAMBP molecules after the removal of KCl and NaCl, and the molar ratio of t-BAMBP to alkali metal was calculated as 3.13. According to Equation (3), the theoretical molar ratio of t-BAMBP to alkali metal should be 4:1. As can be seen, the t-BAMBP/metal molar ratio in the solid compound was greater than the

theoretical ratio, so it was speculated that excessive alkali metal led to the formation of the solid compound.

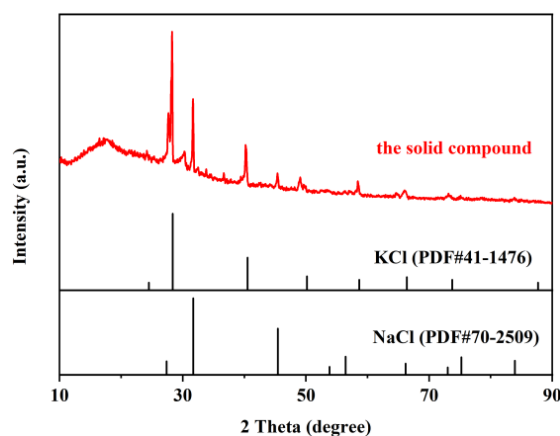


Figure 7. XRD patterns of the solid compound dried at 120 °C.

Table 2. Chemical composition of the solid compound.

Material	Preprocessing	Element Mass Percentage (%)			
Solid compound	Without scrubbing	Na	K	Rb	Cs
	After scrubbing	2.35	2.66	1.39	8.23
	After scrubbing	Na	K	Rb	Cs
		/	0.16	0.32	8.05

In order to confirm this speculation, we compared the state of the organic phase under different t-BAMBP/metal molar ratios. In the experiments, the t-BAMBP/metal molar ratio of the organic phase was changed by changing the O/A ratio of the extraction process, and the other conditions were 1 mol/L NaOH, 1 mol/L t-BAMBP, and a 2 min contact time. As shown in Table 3, when the molar ratio of t-BAMBP molecules to alkali metal was less than 4, the solid compound appeared, and when the t-BAMBP/metal molar ratio decreased, the amount of solid compound increased.

Table 3. States of organic phases under different t-BAMBP/metal molar ratios.

O/A	Raffinate Concentration (g/L)			Organic Concentration (g/L)			Molar Ratio of t-BAMBP/Metal	Appearance of the Solid Compound
	K	Rb	Cs	K	Rb	Cs		
1:3	77.13	5.53	2.34	15.16	3.04	16.12	1.84	Large quantity
1:2	74.66	4.96	1.87	15.04	3.16	11.67	1.96	Large quantity
1:1	74.23	4.01	0.84	7.95	2.53	6.87	3.52	Small quantity
2:1	70.76	2.73	0.39	5.71	1.90	3.66	5.10	No
3:1	69.25	2.11	0.31	4.31	1.48	2.47	6.85	No

However, the above analysis does not explain the formation of the solid compound; the relationship between the molar ratio of t-BAMBP molecules to alkali metal and the formation of the solid compound needs to be further verified.

### 3.4.2. Infrared Spectral Analysis

Infrared (IR) spectroscopy is an effective method for analyzing organic matter and can be used to identify the functional groups in a molecule. In order to determine the difference between the solid compound and the fresh organic phase, three organic phases (solid compound, loaded organic phase, and organic phase) were analyzed by infrared spectrometry. The organic phase consisted of 30 vol% t-BAMBP and 70 vol% sulfonated

kerosene, the loaded organic phase was obtained from the organic phase through the single extraction process, and the solid compound was obtained in the multi-stage extraction process. The results are shown in Figure 8. The stretching vibration bands of  $\sigma_{C-H}$  are in the range of 2845 to 2975  $\text{cm}^{-1}$ . The characteristic peaks of  $\sigma_{O-H}$  and  $\sigma_{Ar-H}$  are around 3540 and 3030  $\text{cm}^{-1}$ , respectively [25]. Compared with the organic phase, the stretching vibration bands of  $\sigma_{O-H}$  in the loaded organic showed a significant decrease in intensity, indicating the ion exchange reaction between hydrogen ions in the phenol hydroxyl group and alkali metal ions. Meanwhile, the characteristic peak of  $\sigma_{O-H}$  in the solid compound shifted to a lower wavelength with an increase in intensity, indicating the formation of hydrogen bonds in the solid compound. Wang et al. [35] studied the effect of hydrogen bonding on the melting point of organic matter and concluded that the formation of hydrogen bonds increases the melting point of organic matter due to an increase in intermolecular forces.

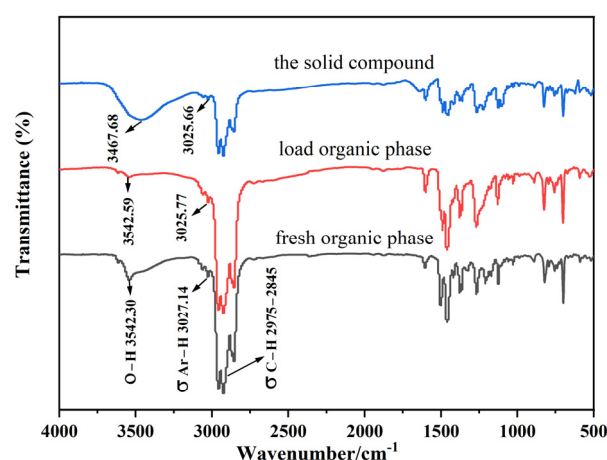


**Figure 8.** Infrared spectra of the organic phase, loaded organic phase, and solid compound.

Based on the above analysis, due to the formation of hydrogen bonds in the extraction complex, the amount of hydrogen bonds increased with the increase in alkali metals extracted into the organic phase, which led to an increase in the melting point of organic matter. Therefore, the solid compound appeared in the organic phase.

#### 4. Conclusions

In this study, cesium and rubidium were successfully separated from a feed solution with high concentrations of potassium and sodium. The main conclusions are summarized as follows:

- (1) The optimal extraction conditions for separating Cs and Rb from high concentration of K and Na were as follows: 1 mol/L t-BAMBP extractant (in sulfonated kerosene), 0.5 mol/L NaOH, O/A ratio of 3:1, and 1 min contact time. More than 99% of Cs and 98% of Rb were recovered by a five-stage countercurrent extraction.
- (2) The organic phase was scrubbed with deionized water at an O/A ratio of 2:1, and 99.32% of K was removed after five-stage countercurrent scrubbing. In the stripping stage, 0.5 mol/L HCl solution was sufficient to strip rubidium and cesium, and after two-stage countercurrent stripping at an O/A ratio of 3:1, more than 99% of Cs and Rb were stripped from the organic phase.
- (3) A solid compound may appear when the t-BAMBP/metal molar ratio in the organic phase is less than 4. The amount of solid compound increased with a decrease in the t-BAMBP/metal molar ratio.
- (4) The formation of the solid compound is related to intermolecular hydrogen bonds, resulting in an increased melting point of the organic phase.

**Supplementary Materials:** The following supporting information can be downloaded at: <https://www.mdpi.com/article/10.3390/separations10010042/s1>, Table S1: The top ten journal articles that related to the separation of cesium and rubidium in recent year.

**Author Contributions:** J.X.: conceptualization, investigation, writing—original draft. K.L.: investigation, validation. Z.S.: visualization, investigation. C.M.: validation, formal analysis. S.L.: project administration, resources. Z.Y.: validation. R.M.: funding acquisition, writing—reviewing and editing. All authors have read and agreed to the published version of the manuscript.

**Funding:** This research was funded by the National Natural Science Foundation of China (Grant No. 52174354).

**Data Availability Statement:** Not applicable.

**Acknowledgments:** The authors acknowledge funding support from the National Natural Science Foundation of China (Grant No. 52174354).

**Conflicts of Interest:** The authors declare no conflict of interest.

## References

1. Fang, D.Z.; Wang, Y.P.; Liu, H.N.; Zhang, H.F.; Ye, X.S.; Li, Q.; Li, J.; Wu, Z.J. Efficient extraction of Rb<sup>+</sup> and Cs<sup>+</sup> by a precipitation flotation process with ammonium phosphowolframate as precipitant. *Colloids Surf. A* **2021**, *608*, 125581. [[CrossRef](#)]
2. Ivanova, Z.G.; Zavadil, J.; Kostka, P.; Djouama, T.; Reinfelde, M. Photoluminescence properties of Er-doped Ge-In(Ga)-S glasses modified by caesium halides. *Phys. Status Solidi B* **2017**, *254*, 1600662. [[CrossRef](#)]
3. Xu, X.L.; Singh, H.P.; Wang, L.; Qi, D.L.; Poulos, B.K.; Abramson, D.H.; Jhanwar, S.C.; Cobrinik, D. Rb suppresses human cone-precursor-derived retinoblastoma tumours. *Nature* **2014**, *514*, 385–388. [[CrossRef](#)] [[PubMed](#)]
4. Saliba, M.; Matsui, T.; Domanski, K.; Seo, J.; Ummadisingu, A.; Zakeeruddin, S.M.; Correa-Baena, J.; Tress, W.R.; Abate, A.; Hagfeldt, A.; et al. Incorporation of rubidium cations into perovskite solar cells improves photovoltaic performance. *Science* **2016**, *354*, 206–209. [[CrossRef](#)] [[PubMed](#)]
5. Harikesh, P.C.; Mulmudi, H.K.; Ghosh, B.; Goh, T.W.; Teng, Y.T.; Thirumal, K.; Lockrey, M.; Weber, K.; Koh, T.M.; Li, S.Z.; et al. Rb as an Alternative Cation for Templating Inorganic Lead-Free Perovskites for Solution Processed Photovoltaics. *Chem. Mater.* **2016**, *28*, 7496–7504. [[CrossRef](#)]
6. Chen, Q.; Peng, C.G.; Du, L.; Hou, T.; Yu, W.J.; Chen, D.; Shu, H.; Huang, D.J.; Zhou, X.Q.; Zhang, J.Y.; et al. Synergy of mesoporous SnO<sub>2</sub> and RbF modification for high-efficiency and stable perovskite solar cells. *J. Energy Chem.* **2022**, *66*, 250–259. [[CrossRef](#)]
7. Zabeti, M.; Gupta, K.; Raman, G.; Lefferts, L.; Schallmoser, S.; Lercher, J.A.; Seshan, K. Aliphatic Hydrocarbons from Lignocellulose by Pyrolysis over Cesium-Modified Amorphous Silica Alumina Catalysts. *ChemCatChem* **2015**, *7*, 3386–3396. [[CrossRef](#)]
8. Formichella, V.; Camparo, J.; Tavella, P. Mitigation of Lamplight-Induced Frequency Jumps in Space Rubidium Clocks. In *IEEE Transactions on Ultrasonics, Ferroelectrics, and Frequency Control*; IEEE: Piscataway, NJ, USA, 2018; Volume 65, pp. 911–918. [[CrossRef](#)]
9. Zhang, X.F.; Aldahri, T.; Tan, X.M.; Liu, W.Z.; Zhang, L.Z.; Tang, S.W. Efficient co-extraction of lithium, rubidium, cesium and potassium from lepidolite by process intensification of chlorination roasting. *Chem. Eng. Process. Process Intensif.* **2020**, *1477*, 107777. [[CrossRef](#)]
10. Zhang, X.F.; Qin, Z.F.; Aldahri, T.; Rohani, S.; Ren, S.; Liu, W.Z. Separation and recovery of cesium sulfate from the leach solution obtained in the sulfuric acid baking process of lepidolite concentrate. *Hydrometallurgy* **2021**, *199*, 105537. [[CrossRef](#)]
11. Jeppesen, T.; Shu, L.; Keir, G.; Jegatheesan, V. Metal recovery from reverse osmosis concentrate. *J. Clean. Prod.* **2009**, *17*, 703–707. [[CrossRef](#)]
12. Yan, Q.X.; Li, X.H.; Wang, Z.X.; Wu, X.F.; Guo, H.J.; Hu, Q.Y.; Peng, W.; Wang, J.X. Extraction of valuable metals from lepidolite. *Hydrometallurgy* **2012**, *117–118*, 116–118. [[CrossRef](#)]
13. Wang, J.L.; Zhuang, S.T. Removal of cesium ions from aqueous solutions using various separation technologies. *Rev. Environ. Sci. Biotechnol.* **2019**, *18*, 231–269. [[CrossRef](#)]
14. Jandová, J.; Dvořák, P.; Formánek, J.; Vu, H.N. Recovery of rubidium and potassium alums from lithium-bearing minerals. *Hydrometallurgy* **2012**, *119–120*, 73–76. [[CrossRef](#)]
15. Liu, J.L.; Yin, Z.L.; Li, X.H.; Hu, Q.Y.; Liu, W. A novel process for the selective precipitation of valuable metals from lepidolite. *Miner. Eng.* **2019**, *135*, 29–36. [[CrossRef](#)]
16. Naidu, G.; Nur, T.; Loganathan, P.; Kandasamy, J.; Vigneswaran, S. Selective sorption of rubidium by potassium cobalt hexacyano-ferrate. *Sep. Purif. Technol.* **2016**, *163*, 238–246. [[CrossRef](#)]
17. Lian, L.S.; Zhang, S.Y.; Ma, N.; Dai, W. Well-designed a novel phosphomolybdic-acid@PCN-224 composite with efficient simultaneously capture towards rubidium and cesium ions. *Polyhedron* **2021**, *207*, 115402. [[CrossRef](#)]
18. Wang, Z.; Zhang, A.Y.; Su, J.Y.; Chen, R.R. Selective adsorption of potassium and rubidium by metal-organic frameworks supported supramolecular materials. *J. Radioanal. Nucl. Chem.* **2021**, *329*, 359–370. [[CrossRef](#)]

19. Wang, J.L.; Zhuang, S.T.; Liu, Y. Metal hexacyanoferrates-based adsorbents for cesium removal. *Coord. Chem. Rev.* **2018**, *374*, 430–438. [[CrossRef](#)]
20. Xu, C.; Wang, J.C.; Chen, J. Solvent Extraction of Strontium and Cesium: A Review of Recent Progress. *Solvent Extr. Ion Exch.* **2012**, *30*, 623–650. [[CrossRef](#)]
21. Jagasia, P.; Mohapatra, P.K.; Dhama, P.S.; Patil, A.B.; Adya, V.C.; Sengupta, A.; Gandhi, P.M.; Watal, P.K. Studies on the radiolytic stability of newly developed solvent systems containing four calix-crown-6 ligands for radio-cesium recovery. *J. Radioanal. Nucl. Chem.* **2014**, *302*, 1087–1093. [[CrossRef](#)]
22. Huang, D.F.; Zheng, H.; Liu, Z.Y.; Bao, A.M.; Li, B. Extraction of rubidium and cesium from brine solutions using a room temperature ionic liquid system containing 18-crown-6. *Pol. J. Chem. Technol.* **2018**, *20*, 40–46. [[CrossRef](#)]
23. Liu, S.M.; Liu, H.H.; Huang, Y.J.; Yang, W.J. Solvent extraction of rubidium and cesium from salt lake brine with t-BAMBP-kerosene solution. *Trans. Nonferrous. Met. Soc. China* **2015**, *25*, 329–334. [[CrossRef](#)]
24. Li, Z.; Pranolo, Y.; Zhu, Z.W.; Cheng, C.Y. Solvent extraction of cesium and rubidium from brine solutions using 4-tert-butyl-2-( $\alpha$ -methylbenzyl)-phenol. *Hydrometallurgy* **2017**, *171*, 1–7. [[CrossRef](#)]
25. Xing, P.; Wang, G.D.; Wang, C.Y.; Ma, B.Z.; Chen, Y.Q. Separation of rubidium from potassium in rubidium ore liquor by solvent extraction with t-BAMBP. *Miner. Eng.* **2018**, *121*, 158–163. [[CrossRef](#)]
26. Zhang, A.Y.; Hu, Q.H. Removal of cesium by countercurrent solvent extraction with a calix[4]crown derivative. *Sep. Sci. Technol.* **2017**, *52*, 1670–1679. [[CrossRef](#)]
27. Mohite, B.S.; Burungale, S.H. Separation of Rubidium from Associated Elements by Solvent Extraction with Dibenzo-24-crown-8. *Anal. Lett.* **1999**, *32*, 173–183. [[CrossRef](#)]
28. Zhang, X.F.; Qin, Z.F.; Aldahri, T.; Ren, S.; Liu, W.Z. Solvent extraction of rubidium from a sulfate solution with high concentrations of rubidium and potassium using 4-tert-butyl-2-( $\alpha$ -methylbenzyl)-phenol. *J. Taiwan Inst. Chem. E* **2020**, *116*, 43–50. [[CrossRef](#)]
29. Xing, P.; Wang, C.Y.; Chen, Y.Q.; Ma, B.Z. Separation of potassium from sodium in alkaline solution by solvent extraction with 4-tert-butyl-2-( $\alpha$ -methylbenzyl) phenol. *J. Cent. South Univ.* **2021**, *28*, 2003–2009. [[CrossRef](#)]
30. Wang, J.W.; Che, D.H.; Qin, W. Extraction of rubidium by t-BAMBP in cyclohexane. *Chin. J. Chem. Eng.* **2015**, *23*, 1110–1113. [[CrossRef](#)]
31. Chen, W.S.; Lee, C.H.; Chung, Y.F.; Tien, K.W.; Chen, Y.J.; Chen, Y.A. Recovery of Rubidium and Cesium Resources from Brine of Desalination through t-BAMBP Extraction. *Metals* **2020**, *10*, 607. [[CrossRef](#)]
32. Gao, L.; Ma, G.H.; Zheng, Y.X.; Tang, Y.; Xie, G.S.; Yu, J.W.; Liu, B.X.; Duan, J.Y. Research Trends on Separation and Extraction of Rare Alkali Metal from Salt Lake Brine: Rubidium and Cesium. *Solvent Extr. Ion Exch.* **2020**, *38*, 753–776. [[CrossRef](#)]
33. Ross, W.J.; White, J.C. Determination of Cesium and Rubidium after Extraction with 4-sec-Butyl-2( $\alpha$ -methylbenzyl) phenol. *Anal. Chem.* **1964**, *36*, 1998–2000. [[CrossRef](#)]
34. Lv, Y.W.; Ma, B.Z.; Liu, Y.B.; Wang, C.Y.; Zhang, W.J.; Chen, Y.Q. Selective extraction of cesium from high concentration rubidium chloride leach liquor of lepidolite. *Desalination* **2022**, *530*, 115673. [[CrossRef](#)]
35. Wang, J.H.; Shen, C.; Liu, Y.C.; Luo, J.; Duan, Y.J. Effects of hydrogen bond on the melting point of azole explosives. *J. Mol. Struct.* **2018**, *1163*, 54–60. [[CrossRef](#)]

**Disclaimer/Publisher’s Note:** The statements, opinions and data contained in all publications are solely those of the individual author(s) and contributor(s) and not of MDPI and/or the editor(s). MDPI and/or the editor(s) disclaim responsibility for any injury to people or property resulting from any ideas, methods, instructions or products referred to in the content.